Removal of strontium from aqueous solutions and synthetic seawater using resorcinol formaldehyde polycondensate resin

T. Nur, P. Loganathan, J. Kandasamy, S. Vigneswaran

Faculty of Engineering, University of Technology Sydney (UTS), P.O. Box 123, Broadway, NSW 2007, Australia

*Corresponding author. Tel.:+61 2 95142641, fax: +61 2 95142633.

Email: s.vigneswaran@uts.edu.au

Research Highlights

- Resorcinol formaldehyde resin had high Sr adsorption capacity at pH 7.5-8.5.

- Batch adsorption data fitted to Langmuir model and column data to Thomas model.

- Cation adsorption capacities decreased in the order Sr > Ca > Mg > K.

- Seawater concentrations of Ca and Mg reduced Sr adsorption capacity.

Abstract

Strontium (Sr) is a valuable metal found in abundance in seawater. However, its recovery from seawater has received little attention despite its many industrial applications. Batch and column adsorption experiments were conducted on the removal of Sr by resorcinol formaldehyde (RF) resin in the presence of co-existing cations at pH 7.5-8.5, where maximum adsorption was found. Batch adsorption capacities of cations followed the decreasing order of Sr > Ca > Mg > K, the order being the same as that of reduction of negative zeta potential. The adsorption data for Sr, Ca and Mg satisfactorily fitted to the Langmuir adsorption model with maximum adsorption capacities of 2.28, 1.25 and 1.15 meq/g, respectively. Selectivity coefficients for Sr with respect to other metals showed that Sr was selectively adsorbed on RF. Column adsorption data for Sr only solution fitted well to the Thomas model. Sr adsorption capacity in the presence of seawater concentrations of Ca, Mg, K and Na was reduced in both batch and column experiments with highest effect from Ca and Mg. However, if Ca and Mg are removed prior to RF adsorption process by precipitation, the negative effect of these ions on Sr removal can be significantly reduced.

Keywords: adsorption, radioactive waste, resorcinol formaldehyde, seawater, strontium, zeta potential

1. Introduction

Seawater is becoming an important source of several valuable mineral resources because of the depletion of high-grade mineral ores on land and recent problems associated with land-based industries resulting from sustainable water and energy demand and environmental issues [1]. Due to its large reserve, seawater is an attractive resource for valuable minerals such as lithium, uranium, rubidium, and strontium (Sr) despite their very low concentrations. Among these valuable minerals, Sr is one of the most abundant minerals in seawater with an average concentration of 6-7 mg/L [2]. Strontium, which is an alkaline earth metal, has many industrial applications, such as in ceramic ferrite magnets, ceramics, glass and pyrotechnics industries, fluorescent lights and fire-works, and also for drilling mud in the oil and gas industries [1,3]. To date, however, the recovery of Sr from seawater has received little attention despite its many industrial applications.

Moreover, the removal of Sr from radioactive waste water is a very critical issue as it is considered one of the most dangerous radionuclides to human health due to its high solubility, transferability, and easy assimilation [4,5]. Strontium has four major naturally occurring stable isotopes: ^{84}Sr, ^{86}Sr, ^{87}Sr and ^{88}Sr in addition to 31 unstable isotopes and the longest-lived unstable isotope is ^{90}Sr with a half-life of 28.9 years. The ^{90}Sr isotope is a beta-emitter that genetically affects seawater organisms and ultimately causes harm to humans [6]. Removing radioactive Sr from seawater is also important particularly since the Fukushima nuclear plant accident in 2011, which led to serious seawater contamination by radioactive strontium ^{90}Sr [7,8].

Strontium genetically impacts on seawater organisms and eventually causes serious damage to humans. In countries like the USA, Jordan and Japan, Sr contamination in groundwater and other water sources has been reported and the United States Environmental Protection Agency (U.S. EPA) has recommended a permissible limit of 4.0 mg/L of Sr in drinking water [9]. High Sr concentrations in drinking water sources may potentially lead to

many diseases increasing, including neurological disorders ranging from learning disabilities to severe mental retardation [10]. It is therefore important to develop appropriate removal techniques for the removal of Sr from water both to decontaminate waters and to recover Sr for beneficial uses.

Of the various methods for removing Sr such as solvent extraction [11], adsorption [12,13], ion exchange [14], electrocoagulation [15], and membrane filtration [16], adsorption/ion exchange is a promising method for removing Sr from seawater and radioactive wastewaters because of its potential to separate Sr from seawater despite the low concentration levels of this metal, low cost, and a simple process to implement with less chemical waste production. As ion exchange is one type of adsorption process which leads to adsorption of ions [17], in this paper it is discussed under the general process of adsorption. Different studies have been conducted to investigate Sr adsorption using various adsorbents such as hydrous ferric oxide [18], dolomite [19], strontium-ion imprinted hybrid gel [20], alginate-based biosorbent [21] and titanosilicate [22]. Not all adsorbents, however, were found to have high adsorption capacities. Moreover, most of these Sr adsorption studies were conducted in batch experiments and not in column experiments which are more appropriate for practical application.

Resorcinol formaldehyde (RF) resin is an effective phenolic resin which is formed by the polycondensation of resorcinol and formaldehyde in alkaline solution [23]. Commercial phenol formaldehyde resins – similar to RF resin - were utilised to treat low and high level alkaline radioactive wastes [24], as well as laboratory synthesised phenol formaldehyde resins for the removal of both Cs and Sr from radioactive wastewaters [25]. Previous research reported that the phenol formaldehyde resins that are similar to RF resin were generally conditioned with alkaline solutions. This is because the main functional weakly acidic phenolic –OH groups of the resin responsible for ion exchange were expected to fully realise their ion-exchange properties only if the –OH groups were ionised to the highest extent which occurs in alkaline solutions [23]. It was reported that RF resin could be used to simultaneously adsorb Sr along

4

with Cs from radioactive waste solutions [25], but Banerjee et al. [26] found that the RF resin used in their study was highly selective for the removal of Cs compared to Sr from simulated radioactive waste solution. However, no detailed study has been done on Sr removal and recovery from seawater using RF resin, especially in the presence of co-ions using both batch and column methods. The concentration of Cs ($4\text{-}50 \times 10^{-5}$ M) is much higher than that of Sr ($3\text{-}15 \times 10^{-7}$ M) in radioactive wastewater [27]. Therefore, Cs was preferentially adsorbed on RF. However, in seawater, the opposite is expected to occur because Sr concentration (1×10^{-4} M) is much higher than that of Cs (6×10^{-9} M) [1].

The objectives of this study were to: (i) synthesise and evaluate the performance of RF resin for Sr adsorption in batch and column adsorption methods; (ii) evaluate the pH effect on Sr adsorption and study the adsorption mechanism using zeta potential measurements; (iii) investigate the effect of co-ions in seawater on Sr adsorption using synthetic seawater in batch and column adsorption methods; and (iv) evaluate the Sr desorption characteristics of the RF resin to obtain useful information on Sr recovery.

## 2. Materials and Method

2.1. Adsorbents

The main adsorbent used in this study was RF resin but four other commercially available adsorbents namely CsTreat, ammonium molybdophosphate (AMP), Zeolite, and Amberlite FPC 3500 were also used to compare their Sr adsorption capacities [28,29]. RF resin was prepared by following the procedure described by Samanta et al. [23] where a mixture of solutions with resorcinol: formaldehyde: NaOH: H_2O mole ratio of 1:2.5:1.5:50 was used. The dark-red coloured mixed solution was then oven dried at 100˚C for 24 h and the dried reddish brown RF resin was ground and sieved to 0.25 - 0.45 mm particle size. The sieved RF resin was then washed with 1 M HCl to convert RF resin to an acid form (H^+). After that, the resin was washed thoroughly with MQ water to convert it to a neutral form and dried at room temperature

$(24 \pm 1° \text{ C})$ for 24 h. To increase the ion exchange capacity, the H^+ form of the resin was conditioned separately with alkaline solutions of 1 M NaOH, KOH and $Ca(OH)_2$ by shaking 5 g of the resin in 500 mL solution of each of the metal hydroxides separately at 150 rpm for 24 h. Following that, the resin was thoroughly washed with MQ water to remove excess NaOH, KOH and $Ca(OH)_2$ and then dried at room temperature $(24 \pm 1° \text{ C})$ for 24 h and kept stored in air tight containers. The reactions involved in the conditioning of RF resin with the different metal hydroxides are given in Eq. (1,2).

$$R - OH + AOH => R - O - A + H_2O \tag{1}$$

$$2 R - OH + B (OH)_2 => (R - O)_2 - B + 2H_2O \tag{2}$$
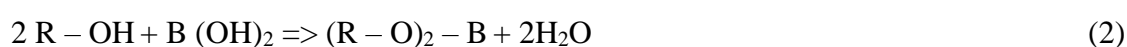
where R is the resorcinol formaldehyde polymer and A is Na^+ or K^+ and B is Ca^{++}.

Based on earlier research on the adsorption of Cs by RF resin, it can be said that the phenolic OH group of the resin is ionised to phenolate ion under alkaline conditions [23,26,30] and then it participates in ion exchange reaction of Sr. The uptake of Sr ions by the resin conditioned with Na^+, K^+, Ca^{++} is shown by similar ion exchange reactions in Eq. (3,4).

$$2 R - O - A + Sr^{++} => (R - O)_2 - Sr + 2A^+ \tag{3}$$

$$(R - O)_2 - B + Sr^{++} => (R - O)_2 - Sr + B^{++} \tag{4}$$
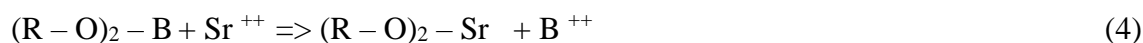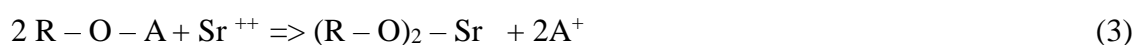
The virgin and the three RF resins conditioned with NaOH, KOH and $Ca(OH)_2$ were used in the adsorption experiments.

2.2. RF resin characterisation

Zeta potential is an important parameter for understanding the mechanism of adsorption as it is the electrical potential close to a particle surface where adsorption of ions from solution phase occurs and it is positively related to the surface charge. The zeta potential values were measured on 0.5 g/L of RF resin suspensions in the presence of 10^{-3} M of NaCl, KCl, $CaCl_2$, $MgCl_2$, or $SrCl_2$ in the pH range of 2.5-10.0 using a Zetasizer nano instrument (Nano ZS

Zen3600, Malvern, UK). Triplicate measurements were made to minimise undesirable biases (with differences between replicates always being less than 5%) and the average value was used for data analyses.

RF resin was also characterised using X-ray diffraction (XRD) and Fourier transform infrared (FTIR) spectroscopy. The FTIR pattern was obtained using a Miracle-10 Shimadzu FTIR spectrometer. The spectra were obtained at 4 cm^{-1} resolution by measuring the absorbance from 400 to 4000 cm^{-1} using a combined 40 scans. XRD was carried out using a PANalytical Empyrean instrument operated at 60-kV with Cu-Ka1 radiation on powdered samples of RF resin.

Ion exchange capacity of the RF resin was measured using two methods [23,28]. In both methods, the RF was equilibrated with known concentrations of NaOH and NaCl and the amounts of NaOH consumed in the ion exchange reaction were determined by titrating the remaining NaOH with 0.1 M HCl using phenolphthalein indicator. The measurements were made in triplicate and the average values were recorded.

2.3. Feed solutions and chemical analysis

Feed solutions were prepared using analar grade chemicals - KCl, NaCl, $CaCl_2$, $MgCl_2$ and $SrCl_2$ (Sigma-Alrich) - at pH 7.5- 8.5. Sr, K, Na, Ca, and Mg concentrations were determined using Microwave Plasma - Atomic Emission Spectroscopy (MP-AES) (Agilent 4100).

2.4. Batch adsorption experiments

2.4.1. Sr adsorption by different RF resins

The first batch experiment was conducted with virgin RF resin and RF resin conditioned separately with NaOH, KOH, and $Ca(OH)_2$ at adsorbent doses of 0.1-1.0 g/L and fixed Sr

concentration of 10 mg/L to select the adsorbent having the highest Sr adsorption capacity. The amount of Sr adsorbed at equilibrium, q_e (mg/g), was calculated using Eq. (5).

$$q_e = \frac{(C_0 - C_e)V}{M}$$

(5)

where C_0 = initial concentration of Sr (mg/L); C_e = equilibrium concentration of Sr (mg/L); V = volume of the solution (L); and M = mass of adsorbent (g).

As RF resin conditioned with NaOH had the highest Sr adsorption capacity among the four resins (Fig. S1), the subsequent adsorption experiments were conducted with this resin only.

2.4.2. Sr adsorption by different commercial adsorbents

Equilibrium adsorption experiments were conducted in a set of glass flasks with 100 mL solutions of pH 7.5-8.5 containing Sr at a concentration of 10 mg/L that is approximately the same as the Sr concentration in seawater. Four commercially available adsorbents (CsTreat, AMP, Zeolite and Amberlite FPC 3500) at doses of 0.1 –10 g/L were added to the solutions and agitated as before in a flat shaker to determine their relative Sr adsorption capacities. At the end of the shaking period of 24 h, the samples were filtered and the filtrates were analysed for Sr concentration. The amount of Sr adsorption was calculated using Eq. (5).

2.4.3. K, Ca, and Mg adsorption

The adsorption of K, Ca, and Mg on RF was investigated in experiments similar to that described previously for Sr adsorption with initial cations concentration of 10 mg/L at RF doses of 0.1 –10 g/L. The adsorption data for these metals and Sr were fitted to the Langmuir model (Eq. 6).

$$Q_e = \frac{q_{max}K_L C_e}{1 + K_L C_e} \tag{6}$$

where, Qe = amount of metal adsorption (meq/g) at the equilibrium metal concentration Ce (meq/L), q_{max} = maximum amount of the metal adsorption (meq/g), K_L = Langmuir adsorption constant (L/meq).

2.4.4. Effect of pH on Sr adsorption

The effect of pH on Sr adsorption was investigated by adding 0.05 g RF resin to 100 mL solution containing 10 mg Sr/L and the suspension was shaken in a flat shaker with a shaking speed of 120 rpm at room temperature (24 ± 1 °C) for 24 h. The solutions' pH values were initially set at a range of 2.5 – 10.0 using 0.1 M HCl and 0.1 M NaOH. They were adjusted back to their initial values after a shaking period lasting 4 h. The final pHs at the end of the shaking period were measured. A HQ40d portable pH Meter was used for all pH measurements.

2.4.5. Effect of co-ions in seawater medium on Sr adsorption

Three adsorption experiments were conducted to determine the effect of co-ions on Sr adsorption. The first experiment was conducted in synthetic seawater containing Na (20 g/L), Ca (1 g/L), Mg (2 g/L), K (0.85 g/L) and Sr (10 mg/L) with RF doses of 0.1 – 10 g/L. The second experiment was conducted by keeping the Sr concentration and RF dose fixed at 10 mg/L and 1 g/L, respectively, but Na (20 g/L), Ca (1 g/L), Mg (2 g/L) or K (0.85 g/L) was added individually to separate Sr solutions. To determine the co-ions having the greatest influence on Sr adsorption, the third experiment was undertaken at three concentrations of Ca, Mg and K (10, 20, 40 mg/L) in the presence of a fixed concentration of Sr (10 mg/L) at a RF resin dose of 1 g/L. This experiment is expected to provide information on the effect of different ratios of the concentrations of Sr to co-ions on Sr adsorption. The amount of Sr adsorption was calculated using Eq. (5).

2.4.6. Selectivity of Sr adsorption on RF resin

Another experiment was conducted to investigate the selectivity of Sr adsorption on RF resin when the same concentration of Sr, Ca, Mg and K (10 mg/L) was used at a RF resin dose of 1 g/L. The amount of each metal adsorbed was calculated using Eq. (5). The removal efficiency (%) of a metal ion by RF was determined by dividing the amount adsorbed by the amount initially present and multiplying by 100. The distribution coefficient (K_d) (L/g) of a metal was calculated by dividing the amount of metal adsorbed (meq/g) by the equilibrium concentration of the metal in solution (meq/L) [23,25,28] and the selectivity coefficient of Sr with respect to another metal (K_s) was determined by dividing the K_d of Sr by the K_d of the other metal [31]. The higher the Ks value of Sr, the higher the selectivity of adsorption of Sr with respect to the other metal.

2.5. Column adsorption experiments

The column adsorption experiments were done using a fixed-bed column consisting of a Pyrex glass tube where a stainless-steel sieve was attached to the bottom followed by a layer of glass beads to provide a uniform flow of the solution through the column. A known quantity of RF resin (10 g) was packed above the glass beads in the column consisting of 1.8 cm inner diameter to yield the desired bed height (6 cm). Feed solutions of 10 mg Sr/L with and without co-ions at concentrations that are found to occur in seawater (see section 2.4.5) were pumped upward through the column at a desired filtration velocity (10.6 mL/min, 2.5 m/h) which was controlled by a peristaltic pump. The experiment was deliberately conducted with a shorter bed height to obtain a faster breakthrough of metals. Since a shorter bed height was used, a smaller filtration velocity was used instead of a normally used velocity of 10 m/h. The effluents at the outlet of the column were collected at regular time intervals and the Sr concentrations were measured. The breakthrough curve shows the loading behaviour of Sr to be removed from the

10

solution in the column and is usually expressed in terms of adsorbed Sr concentration (C_{ad}), inlet Sr concentration (C_o), outlet Sr concentration (C) or normalised concentration defined as the ratio of outlet Sr concentration to inlet Sr concentration (C/C_o) as a function of time. The maximum column adsorption capacity, q_{total} (meq of Sr/g), for a given feed concentration and filtration velocity is equal to the area under the plot of the adsorbed Sr concentration, C_{ad} (C_{ad} = C_o-C) (meq/L) versus effluent time (t, min) and was calculated manually using Microsoft Excel spreadsheet according to Eq. (7).

$$q_{total} = \frac{Q}{1000} \int_{t=0}^{t=total} C_{ad} dt$$

(7)

The breakthrough curves for the co-ions Ca, Mg and K were also determined by measuring their concentrations in the effluent. The amounts of these metals adsorbed on RF were determined using Eq. (7).

Equilibrium Sr uptake q_{eq} (meq/g) or maximum Sr capacity of the column is q_{total} divided by the mass of the adsorbent. The column adsorption data were fitted to the Thomas model (Eq 8) which has been described elsewhere [32].

$$\ln(C_o/C - 1) = k_{Th}q_oM/Q - k_{Th}C_ot$$

(8)

where, k_{Th} is the Thomas rate constant (L/min.meq), q_o is the maximum solid-phase concentration of the solute (meq/g), m_c is the mass of adsorbent in the column (g), and Q is the volumetric flow rate (L/min). k_{Th} and q_o were calculated from the model fit to the data. The accuracy of the model fit to the experimental data was determined by applying error analysis methods such as the sum of the squared error (SSE) and root mean squared error (RMSE) described in the following equations [33].

$$SSE = \sum_{i=1}^{n}(yc - ye)^2$$

(9)

$$RMSE = \sqrt{\sum_{i=1}^{n}[(yc - ye)^2]/n}$$

(10)

2.6. Desorption

Sr desorption experiments were conducted using 1 M and 2 M of NaCl and NaOH as desorbing agents. The RF resin containing the adsorbed Sr was washed with MQ water and used for the desorption experiments. As with the Sr adsorption experiment, 1 g of the RF resin containing adsorbed Sr was added to 100 mL of the desorbing solution and agitated for 4 h and then the supernatant was filtered using 0.12 mm syringe filters. The concentration of Sr in the desorbed solution was measured in the filtrate.

3. Results and discussion

3.1. Characterisation of the materials

The X-ray diffraction analysis showed that the RF resin had no diffraction peaks, indicating that the resin was poorly crystalline (amorphous) as reported previously [34]. The FTIR spectrum of the RF resin is shown in Fig. 1. The broad FTIR absorption band at 2800-3500 cm^{-1} and the peak at 1640 cm^{-1} correspond to the symmetrical and anti-symmetrical stretching vibrations of water molecules with hydrogen bonding and free water, respectively. The absorption peak occurring at 1200 - 1500 cm^{-1} is due to OH bending of the phenolic group and the characteristic of the phenyl group. The band at 1000–1150 cm^{-1} is due to C–O stretching and the peak at 600–800 cm^{-1} is assigned to the presence of aromatic rings. The FTIR pattern with the above characteristic peaks agreed with the previous results of RF resin [34].
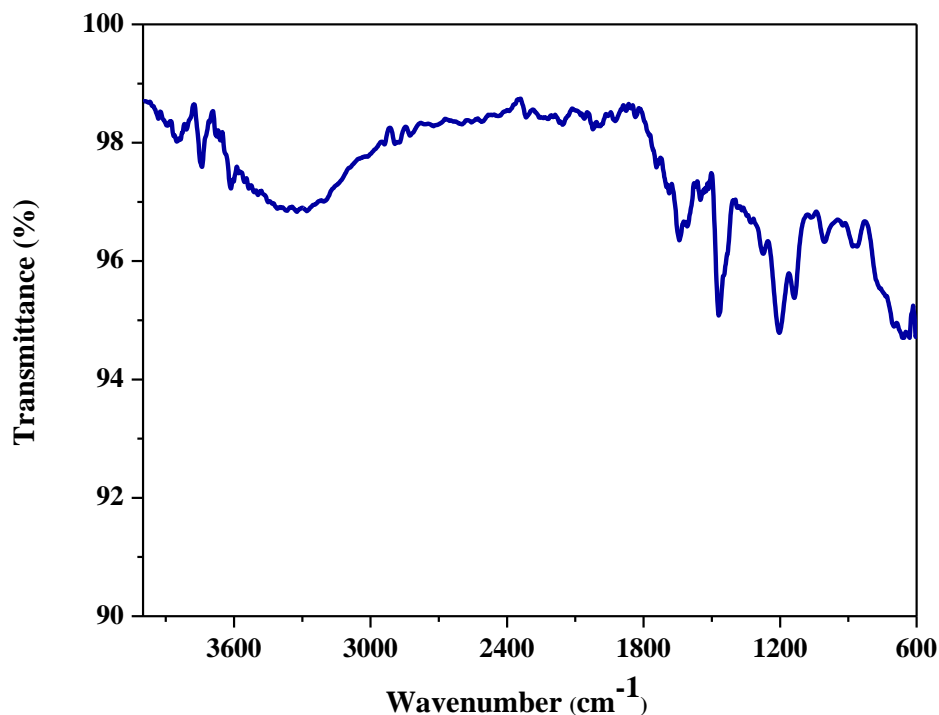
Fig. 1. FTIR spectra of RF resin.

The ion exchange capacity of RF determined by the method of Banerjee et al. [28] was 7.0 ± 0.3 meq/g and that by the method of Samantha et al. [23] was 6.7 ± 0.2 meq/g. These values are very close to the values of 6.0 – 6.9 meq/g reported by others [23,26] for the ion exchange capacity of RF.

3.2. Batch adsorption experiments

3.2.1. Comparison of the adsorption capacities of different RF resins

The results of adsorption experiments with virgin RF resin and RF resins conditioned with three metal hydroxides (1 M NaOH, 1 M KOH, 1 M Ca(OH)$_2$) showed that the NaOH conditioned RF resin had higher Sr removal efficiency than the other resins and virgin RF resin. The Sr removal efficiencies for the RF resins conditioned by these three metal hydroxides were 95%, 50%, and 45%, respectively compared to 40% for the virgin RF resin at the dose of 1 g/L

and initial Sr concentration of 10 mg/L (Fig. S1). Therefore, the RF resin conditioned with NaOH was used in the remaining adsorption experiments.

The higher adsorption capacity of the NaOH conditioned RF towards Sr could be due to the increased number of negatively charged phenolate groups generated in the NaOH system as shown by the zeta potential data (sec 3.2.3). Another study showed that conditioning RF with elevated concentrations of NaOH in the presence of constant Na^+ concentration maintained by a high concentration of $NaNO_3$, increased the adsorption of Cs. This was explained as being due to increased ionisation of phenolic OH groups [23].

3.2.2. Comparison of different adsorbents for Sr adsorption

The adsorption capacities of four commonly used adsorbents were compared with RF in an experiment on adsorption of Sr from a solution with Sr concentration of 10 mg/L. The results showed that of the five adsorbents tested, RF had the highest adsorption capacity (Fig. 2). Approximately 96% removal of Sr was achieved with a resin dose of 1 g/L and the removal efficiency reached 99% and 100% with resin doses of 5 g/L and 10 g/L, respectively. Under the same adsorption conditions, only Amberlite and AMP could achieve about 80% removal efficiency at doses $\geq$ 5g/L.
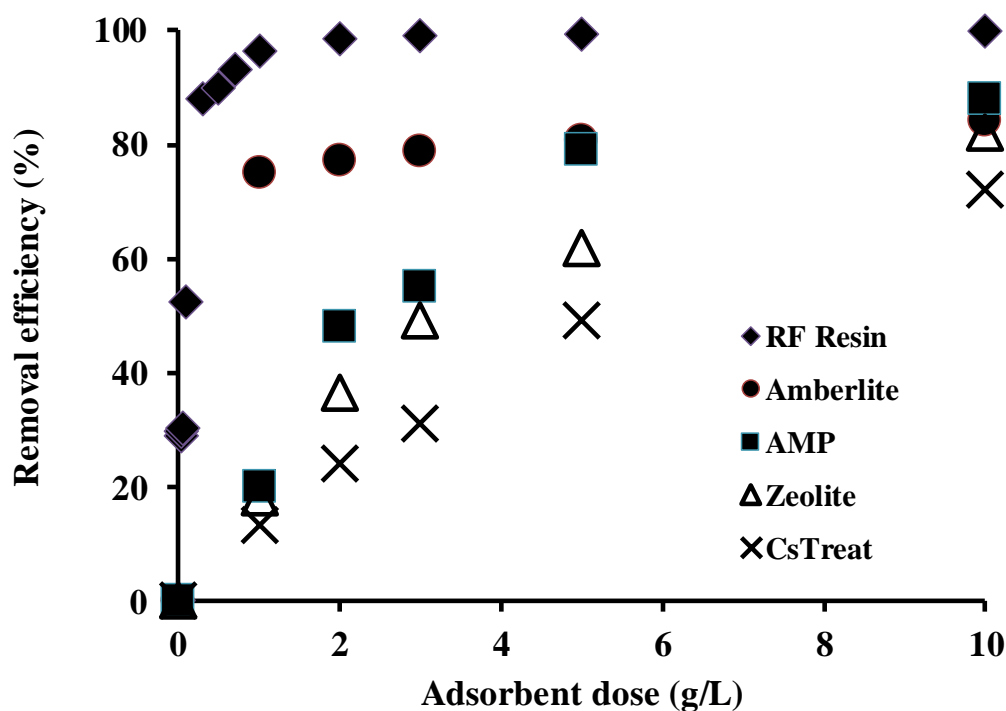
Fig. 2. Sr adsorption isotherm for different adsorbents (initial Sr concentration 10 mg/L, adsorbents doses 1- 10 g/L, pH 7.5 – 8.5)

3.2.3. Effect of pH on Sr adsorption

The adsorption capacity of RF resin in the pH range of 2.5 to 10 revealed that pH exerted a strong effect on Sr adsorption capacity (Fig. 3a). The adsorption capacity remained constant from pH 2.5 to 4.5 and thereafter an abrupt increase was observed up to pH 7.5 and then remained constant up to pH 9.5. Others have also reported that Sr had a sharp increase in adsorption capacity around neutral to slightly alkaline pH on other adsorbents [35,36].

Fig. 3b shows the variation of the zeta potential of RF resin as a function of solution pH and the point of zero charge (PZC, pH at which the net surface charge is zero) of RF to be approximately 3.0. This value agrees with the PZC value of pH 3.2 reported by Sun et al. [37] for phenol-formaldehyde resin that is closely related to the RF. The negative zeta potential, as in the case of the adsorption capacity, also abruptly increased with pH from pH 5 to 8 in the presence of NaCl and KCl. This indicates that the increase in Sr adsorption was due to the increase in the surface negative charge which attracted the positively charged Sr by electrostatic

forces (non-specific adsorpton or outer-sphere complexation [17]). However, Fig 3b also indicated that in the presence of Sr, the zeta potential became less negative above pH 5 compared to RF in the presence of a similar concentration of NaCl (10^{-3} M). The zeta potential value between pH 5 and 7.5 for Sr showed negligible change (Fig. 3 (b)), yet the pH effect on Sr adsorption capacity at this pH range showed a significant increase (Fig. 3a). This suggests that Sr was adsorbed on RF by specific adsorption or inner-sphere complexation [17] and not driven entirely by the coulombic charge balance of the RF surface as dictated by outer-sphere complexation. Inner-sphere complexation may have occurred at neutral surface sites of the RF producing positive surface charges. Such surface complexation mechanism which had less correlation of Sr^{++} adsorption to surface charge development dominated the bonding between Sr^{++} and the FeOOH surface [35]. The positive charges formed on RF surface balanced part of the surface negative charge resulting in a reduction in negative zeta potential.

The sharp increase in adsorption from pH 4.5 to 7.5 was not considered to be due to adsorption of $Sr(OH)^+$ species or surface precipitation of $Sr(OH)_2$ as the formation of these species or precipitation do not occur below pH 11 [35,36]. The high Sr adsorption at high pH was explained as being due to complexation of Sr with the adsorbent's surface OH groups or by the mediation of the high concentration of OH^- ions at high pH [36]. Samanta and Misra [30] explained the higher affinity of Cs towards resorcinol formaldehyde compared to other alkali metals as a consequence of the specific interaction of Cs with the phenolic OH groups of the resin. They stated that this was due to the weak hydration of Cs compared to the strong hydration of the smaller alkali metals. This explanation can also apply to Sr which has the lowest hydrated ionic radius (nm) (Sr 0.180, Ca 0.200, Mg 0.310) [38] and the lowest hydration energy (KJ/mol) (Sr -1524, Ca -1657, Mg -2003) [39] among the alkaline earth metals.

The low adsorption capacity of Sr at low pH is due to fewer negative charges on the RF resin surface as shown by the zeta potential data (Fig. 3b). Also, competition between Sr and the high concentration of protons could be involved in reducing the Sr adsorption capacity.

Because of the high adsorption capacity of Sr at pH 7.5 – 8.5, the rest of the experiments were
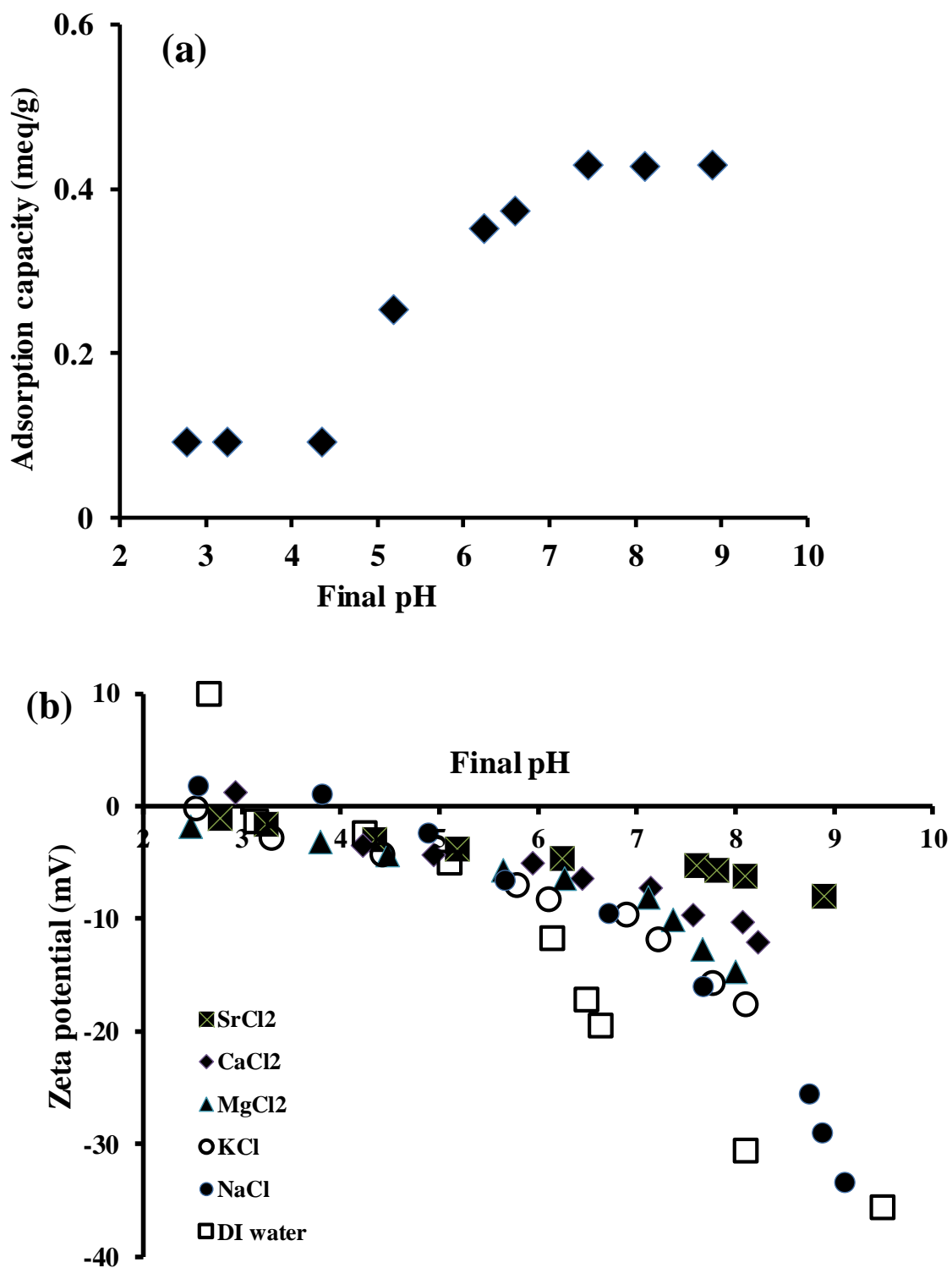
conducted at this pH range.

Fig. 3. Effect of (a) pH on Sr adsorption by RF resin and (b) zeta potential trend as a function of pH for alkali and alkaline earth metals (10^{-3} M) and DI water (RF resin dose 0.5 g/L).

3.2.4. Batch adsorption modelling

The adsorption of Sr on RF showed that the data fitted successfully to the Langmuir model (R^2 = 0.98) (Fig. 4). The maximum adsorption capacity of 2.28 meq/g obtained from the data fit to the Langmuir model is one of the highest Sr adsorption capacity values reported for adsorbents in the literature (Table 1). The data fit to the Langmuir model indicates that the adsorption sites on RF were homogeneous with monolayer adsorption coverage. The adsorption capacity of Sr was much higher than that of the other divalent cations, Ca and Mg and the monovalent cation K (Fig. 4). The adsorption of Ca and Mg also fitted well to the Langmuir adsorption model (R^2 of 0.97 and 0.90, respectively) but the adsorption maxima calculated from the model for Ca of 1.25 meq/g and for Mg of 1.15 meq/g were much lower than that for Sr. This is consistent with the zeta potential data where the surface negative potential on RF decreased in the order Sr > Ca > Mg > K (Fig. 3b). This order reflects the extent of inner-sphere complexation of the cations on the RF surface in addition to the charge difference of the cations (monovalent K vs the divalent ions) controlling the adsorption capacities of the cations.
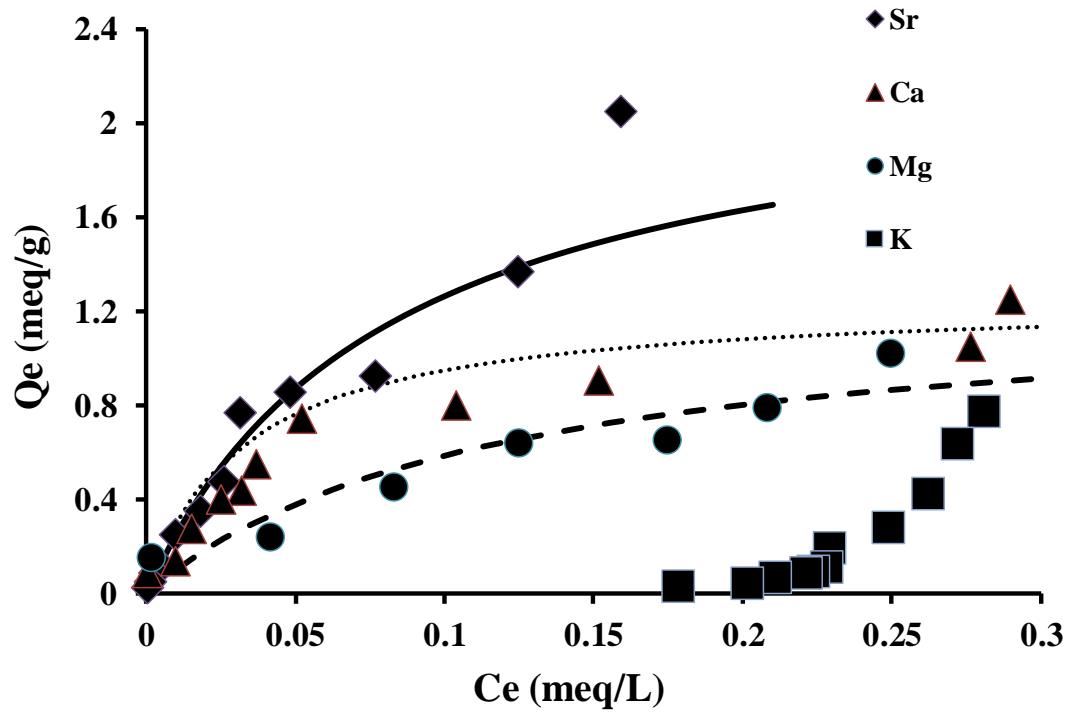
Fig. 4. Langmuir isotherm model fits to data on adsorption of Sr, Ca, Mg and K on RF resin (initial concentration of Sr, Ca, Mg and K 10 mg/L, adsorbent doses of 0.1 – 1.0 g/L, pH =7.5 - 8.5).

Table 1.
Comparison of Langmuir adsorption capacity for Sr on RF resin with that on other adsorbents.

Adsorbent	Experimental conditions	Adsorption capacity (meq Sr/g)	Reference
Bacteriogenic iron oxides	pH 7.0; 293 K	0.01	[40]
Dolomite	pH 5.5; 293 K	0.03	[19]
Hydrous ferric oxide	pH 10.0; 293 K	0.16	[18]
Phosphate-modified montmorillonite	pH 5.0; 298 K	0.29	[4]
Magnetic Fe_3O_4 particles modified sawdust (MCS)	pH 6.7; 293 K	0.29	[41]
Moss biosorbent	pH 6.0; 293 K	0.30	[42]
AMP–PAN	pH 5.0; 293 K	0.36	[29]
Composite magnetic nanoparticles	pH 10.3; 298 K	0.45	[43]
FeOOH (BT9)	pH 11.2; 288 K	0.62	[36]
FeOOH (BT1)	pH 10.5; 293 K	0.75	[35]
Strontium-ion imprinted hybrid gel	pH 11.0; 293 K	1.76	[20]
Titanate nanotubes	pH 8.0; 293 K	2.09	[44]
Alginate microspheres	pH 8.0; 298 K	2.51	[21]
Titanosilicates	pH 7.1; 293 K	3.90	[22]
RF resin	pH 7.5; 298 K	2.28	This study

3.2.5. Co-ions' effect on Sr adsorption

Information on the adsorption behaviour of Sr in the presence of other ions that are present in seawater is useful for the practical application of the adsorption process in recovering Sr from seawater. To obtain this information, an experiment was conducted on Sr adsorption in the presence of the major cations present in seawater such as Na, Ca, Mg and K at concentrations ranging from 10 mg/L to 40 mg/L while that of Sr was fixed at 10 mg/L. The results showed that the adsorption capacity of Sr was not affected by the presence of Na and K even at concentrations four times that of Sr (Fig. 5). However, in the presence of divalent cations, the Sr adsorption reduced by 4, 7, and 10% for Mg concentrations of 10, 20, and 40 mg/L, respectively and 8, 11, and 14% for the corresponding concentrations of Ca. This shows that the divalent Ca and Mg are competing with Sr for adsorption. Between the two ions, Ca reduced Sr adsorption more than Mg did at the same concentration expressed as mg/L which was also found for other Sr adsorbents [44]. With Ca having a higher atomic weight of 40 than Mg of 24, at the same concentration of the two ions expressed as mmol/L, Ca would be even more competitive than Mg for Sr adsorption. Zeta potential data (Fig. 3(b)) where Ca reduced the negative zeta potential more than Mg did (Fig. 3(b)), is consistent with the relative competion outcomes of the two ions on Sr adsorption.

The amounts of Ca and Mg adsorption at the same concentration of Sr of 10 mg/L were 0.37 meq/g and 0.90 meq/g, respectively compared to the adsorption of 0.27 meq/g of Sr (Table S1). However, the initial concentration of Sr expressed as mmol/L was 0.23 meq/L which was much lower than the values of 0.50 meq/L and 0.83 meq/L of Ca and Mg. Therefore, if the adsorption of the metals are compared at the same solution concentration expressed as mmol/L, the difference in the adsorption amounts may not be much different between the metals.
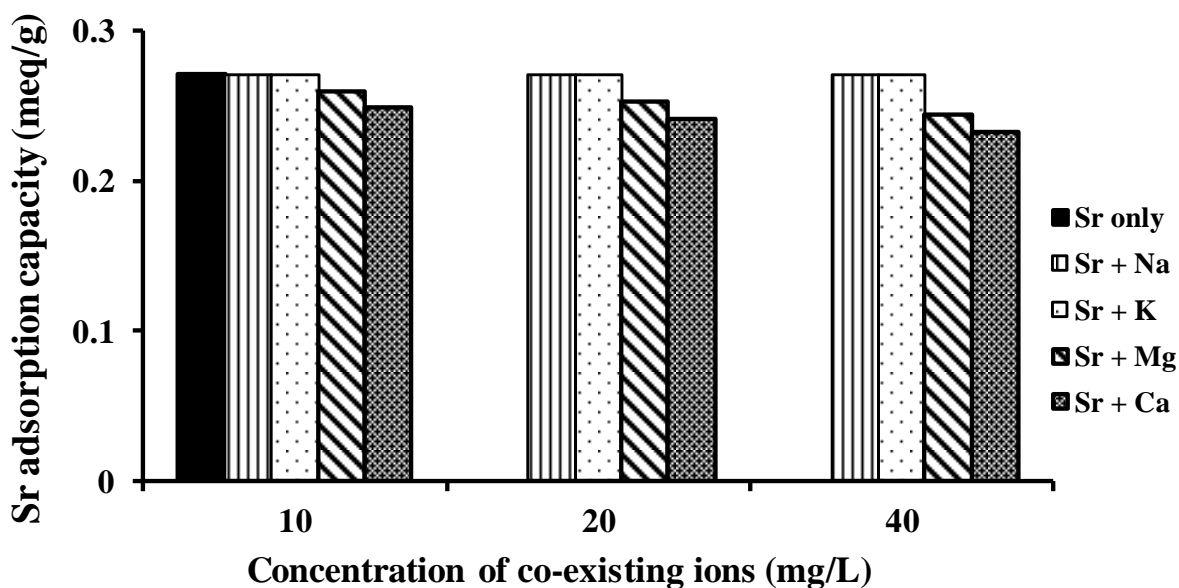
Fig. 5. Effect of different concentrations of co-existing ions on Sr adsorption by RF resin at the dose of 1 g/L (Sr concentration 10 mg/L).

The monovalent K had less effect on Sr adsorption than the divalent Ca and Mg because of the charge difference between the ions and the inner-sphere complexation behaviour of the divalent cations (Fig. 3b). The amount of K adsorbed at the same 10 mg/L solution concentration of K was 0.09 meq/g which is much lower than the amount of Sr adsorbed (0.27 meq/g) confirming that K has less competitive effect on Sr adsorption because K was adsorbed mainly by outer-sphere complexation as shown by the zeta potential results (Table S1).

3.2.6. Selectivity of Sr adsorption on RF resin

The results of the selectivity experiment showed that the removal efficiency of Sr was higher than that of the other metals from solution containing all the four metals together (Fig. 6). The removal efficiency of Sr was about 80%, while those of Ca, Mg and K were 67%, 42% and 1%, respectively. The high removal efficiency of Sr resulted in a high K_d value of 0.079

23

(L/g) for Sr compared to 0.070, 0.054, and 0.001 for Ca, Mg, and K, respectively and selectivity coefficients (K_s) for Sr with respect to Ca, Mg and K of 1.13, 1.46 and 79.0, respectively (Table S2). The K_s values of greater than one indicates that Sr is more selectively adsorbed on RF than the other metal. The selectivity is very much higher with respect to K than the divalent metals, Ca and Mg. However, in determining the relative amounts of the metals' adsorption in practice, the relative concentrations of the metals in solution should also be considered. The selectivity of Sr compared to K is due to the higher valency of Sr(divalent) than K (monovalent) which caused stronger adsorption of Sr. The higher selectivity of Sr in relation to the other divalent alkaline earth metals, Ca and Mg is probably due to Sr having the lowest hydrated ionic radius (nm) (Sr 0.180, Ca 0.200, Mg 0.310) [38] and the lowest hydration energy (KJ/mol) (Sr -1524, Ca -1657, Mg -2003) [39] among the alkaline earth metals. Lower hydrated ionic radius and hydration energy leads to more specific interaction with RF [30]. Zeta potential data showed that the surface negative potential on RF decreased in the order Sr > Ca > Mg > K indicating the order of the strength of adsorption (Fig. 3).
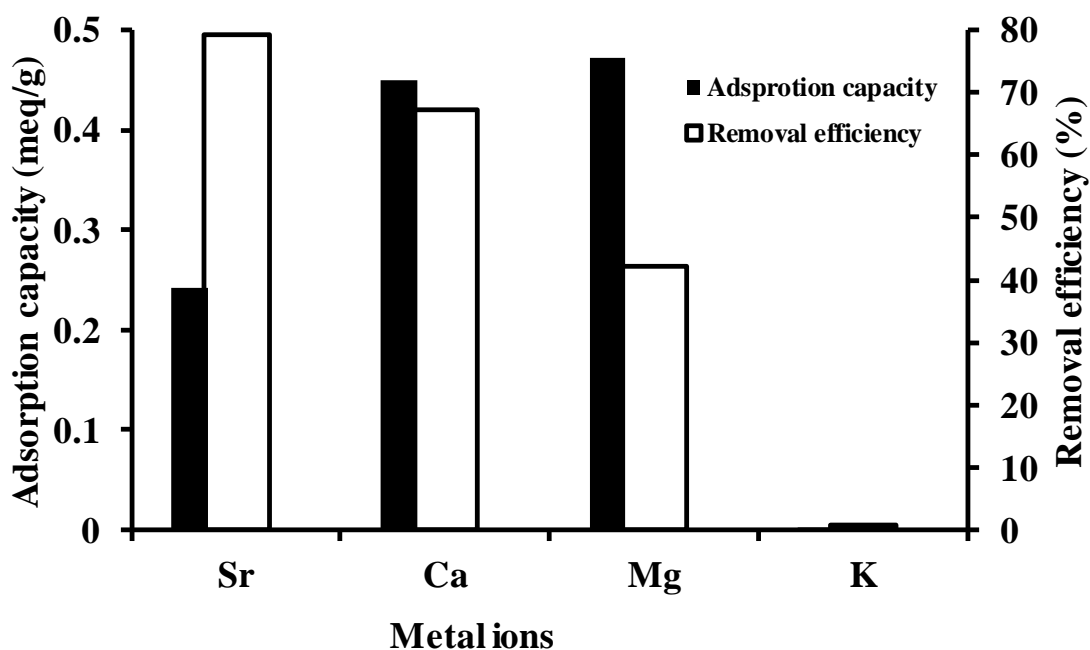
3.2.7. Sr adsorption in seawater medium

To investigate the Sr adsorption behaviour of the RF resin in real seawater conditions, an experiment was conducted on Sr adsorption in synthetic seawater containing Na, Mg, Ca, K, and Sr concentrations (g/L) of 20, 2, 1, 0.85, and 0.01, respectively. The RF resin demonstrated excellent efficiency of nearly 95% Sr recovery at a dose of 1 g/L in deionised water containing 10 mg/L of Sr (Fig. 7a). But the efficiency declined to about 40% in synthetic seawater medium with the same dose of adsorbent. However, the removal efficieny of other metals at the same dose of 1 g/L were < 10% (Fig. S2a) . This indicates that at the same concentration of metals in solution, Sr might be adsorbed selectively compared to other metals. At this RF dose, the amounts of Sr, Ca, Mg and K adsorption were 0.16 meq/g, 3.0 meq/g, 3.0 meq/g and 0.26 meq/g, respectively (Fig. S2b). The higher adsorption capacities of the co-ions compared to Sr

is due to the presence of other metals in the synthetic seawater at much higher concentrations than Sr. Similar results were reported with an alginate microsphere adsorbent where the Sr adsorption capacity was drastically reduced in seawater medium [21].

Fig. 7b shows the Sr adsorption capacity of RF resin when each of the other metals was present individually at the concentrations they are found to occur in seawater. As found previously, Ca and Mg ions competed most with Sr adsorption on RF resin and much of the ion exchange sites were not available for the adsorption of Sr found in much lower concentrations. To avoid this competition, Ca and Mg can be removed prior to the adsorption process by removing them from seawater as $CaCO_3$ and $Mg(OH)_2$ precipitates, respectively [1].
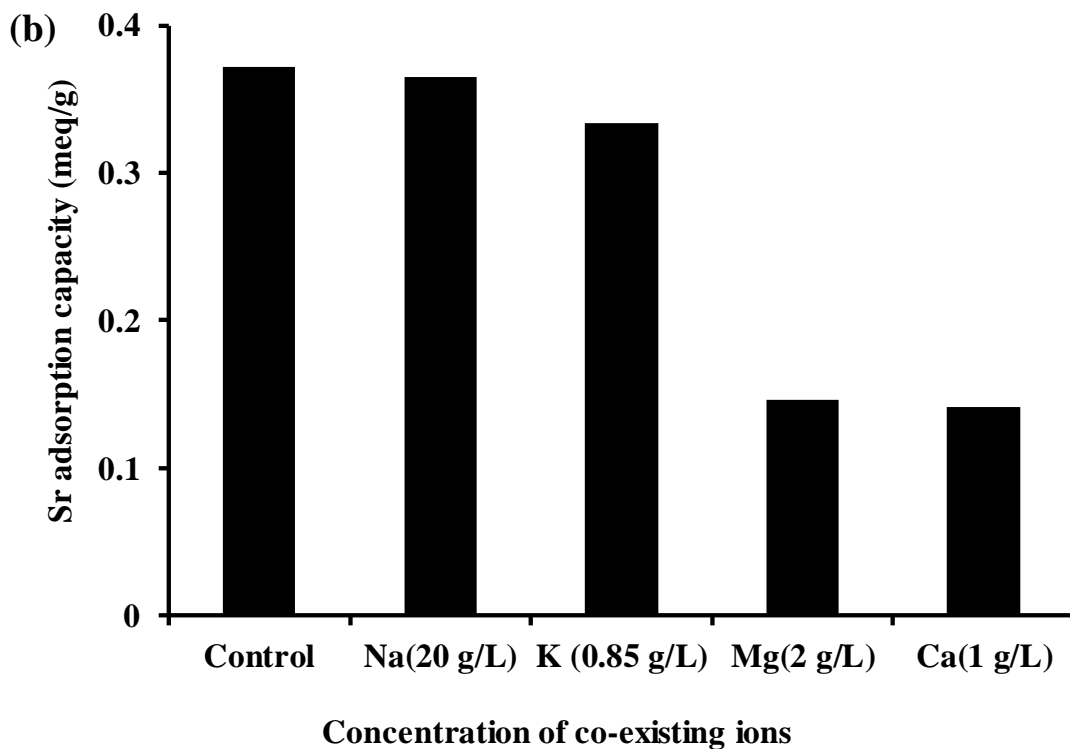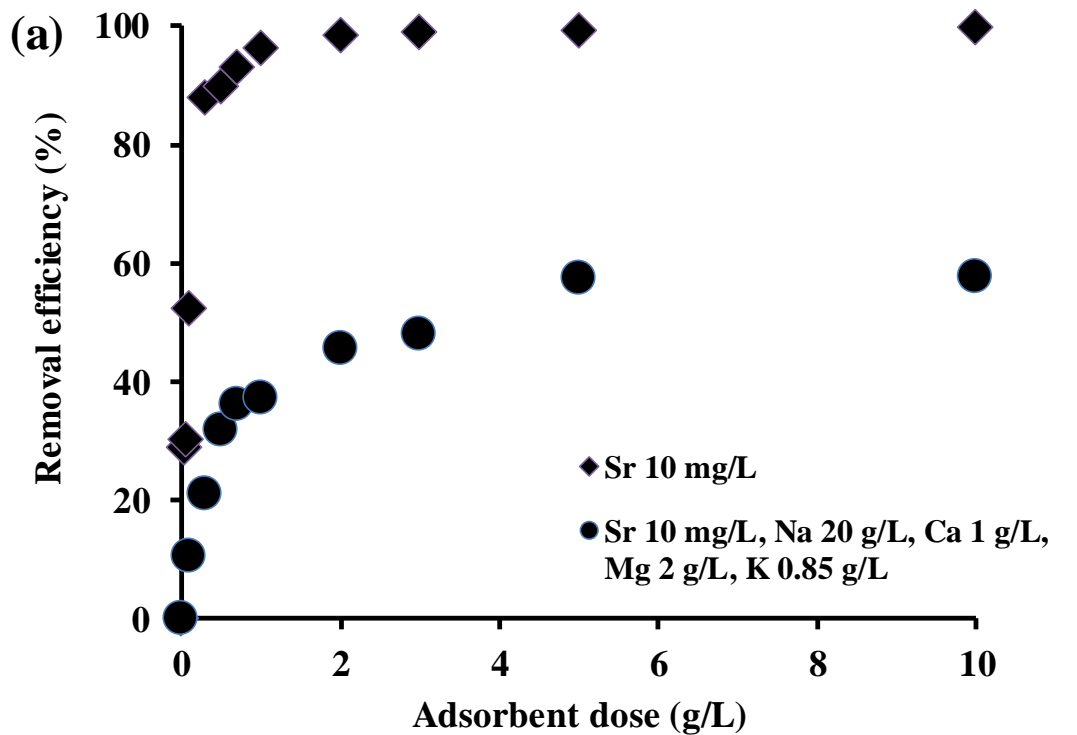
Fig. 7. (a) Removal efficiency of Sr by RF resin in D.I. water and seawater medium with different doses of adsorbent and (b) effect of co-existing seawater cations on Sr adsorption by RF resin (Sr 10 mg/L and adsorbent dose 1 g/L).

3.2.8. Desorption

Desorption of Sr from RF resin was studied to obtain information on the percentage of adsorbed Sr that can be recovered from the desorbed solution. Also, it was necessary to evaluate whether the adsorbent can be reused without any loss of Sr adsorption capacity. Sr desorption efficiency was tested with 1 M and 2 M NaCl and NaOH on a RF sample with adsorbed Sr. The Sr desorption efficiency was found to be higher with 2 M NaCl (100%) than with 1 M NaCl (90%) when 0.1g RF with adsorbed Sr was shaken with 100 mL of NaCl for 3 h. In contrast, even a higher concentration of NaOH (2M) could desorb only 30% of adsorbed Sr (Fig. S3). The inefficiency of the NaOH to desorb Sr is because of the high Sr adsorption in alkaline condition (Fig. 3). The weakly acidic phenolic –OH groups of the resin responsible for ion exchange were expected to fully realise their ion-exchange properties only if the –OH groups were ionised to the highest extent which occurred in alkaline solutions [23]. At a lower pH produced by NaCl (pH 6.5), the adsorption of Sr is weaker and Na at the high concentration of 1 M and 2 M exchanged with Sr and the latter is effectively desorbed.

3.3. Column study

The results from the three column experiments are presented in the form of breakthrough curves in Fig. 8. The first experiment had only Sr in the influent solution at a concentration of 10 mg/L. The second experiment had all the major metals at the concentrations present in seawater in the influent solution along with 10 mg/L of Sr. The third experiment was designed with the same influent concentrations as in experiment 2, but without Ca and Mg present. This experiment is expected to give information on the removal of Sr, if Ca and Mg are removed from the seawater by precipitation as $CaCO_3$ and $Mg(OH)_2$ prior to the RF adsorption process [1]. In the first experiment, the breakthrough of Sr occurred after 417 bed volumes and increasing concentration of Sr was found in the effluent with increasing bed volumes reaching

28

a saturation of the column with Sr after 920 bed volumes (Fig. 8a). On the other hand, in the second experiment the breakthrough commenced from the start of the experiment and column saturation occurred much earlier (Fig. 8b). The breakthrough curve was steeper than in the first experiment. This clearly shows that the co-ions at much higher concentrations than Sr as found in seawater competed with Sr adsorption on RF, thus confirming the batch experimental results. It is interesting to note that in between 200 and 400 bed volumes, C/Co is almost constant. It might indicate preferential exchange of Ca and Mg on RF over Sr in this region. In the third experiment with no Ca and Mg in the influent solution, the breakthrough of Sr occurred after 200 bed volumes and the column became saturated later than in the second experiment (Fig. 8c). The adsorption capacities calculated from the breakthrough curves were 0.50, 0.14, and 0.25 meq/g in the first, second and third experiments, respectively.

The data fitted very satisfactorily to Thomas model when only Sr was present in the influent solution (Fig. 8a). The model fits to the data for Sr adsorption in the presence of other metals in the influent solution were not satisfactory (Fig. 8b, 8c), especially when Ca and Mg were present (Fig. 8b). This may be because of competition of Ca and Mg with Sr for adsorption on RF, which the Thomas model does not take into account. The error analysis of the model fits to the data showed that both the SSE and RMSE were high when other metals were present with Sr, especially Ca and Mg (Table 2). The relationship between model predicted C/Co and experimental C/Co values was very good when only Sr was present (R^2 = 0.93 and slope of the regression line matched the 1:1 line with slope 1) but not satisfactory when other metals were present (R^2 = 0,64 and 0.76) (Table 2, Fig. S5). The adsorption capacities (meq/g) calculated from the model for the corresponding experiments were 0.46, 0.17 and 0.20 (Table 2), respectively. These values are approximately the same as those calculated manually from the breakthrough curves. The adsorption capacity of 0.46 meq/g with the feed solution of only Sr concentration of 10 mg/L is quite low compared to the

Langmuir maximum capacity of 2.28 meq/g determined in the batch experiment. The main reason for this difference is that the flow process used in the column experiment is never at equilibrium unlike in the batch experiments. A similar breakthrough capacity of 0.68 meq/g was reported for zeolite LTA-monoliths when Sr at the same concentration was passed through the monoliths [6].
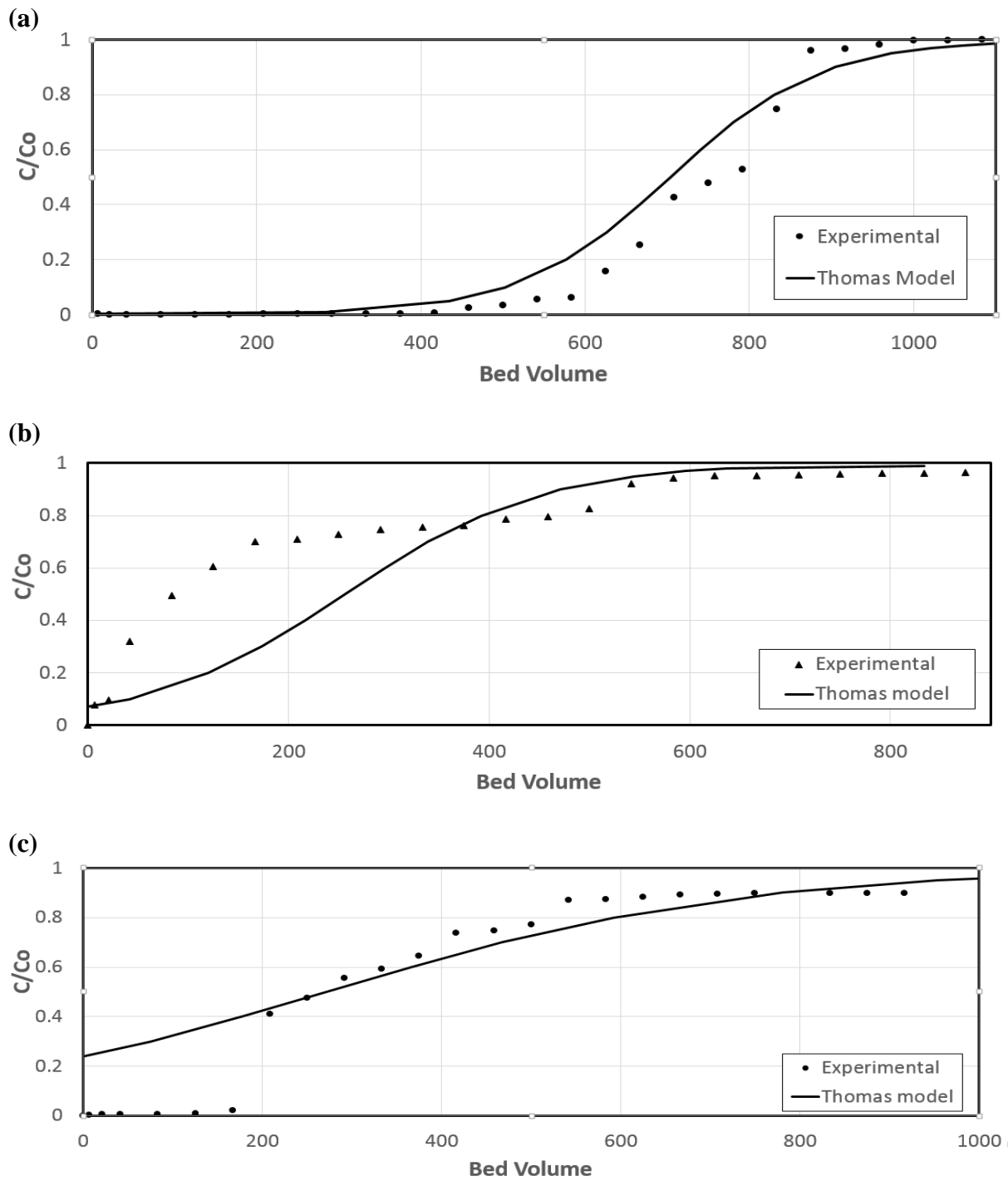
Fig. 8. Breakthrough curves and Thomas model fits to data on column adsorption of Sr with different influents (a) Sr 10 mg/L, (b) Sr 10 mg/L, Na 20 g/L, Ca 1 g/L, Mg 2 g/L, K 0.85 g/L (c) Sr 10 mg/L, Na 20 g/L, K 0.85 g/L, (filtration velocity 2.5 m/h and bed height 6 cm).

The breakthrough curves for the co-ions in the second experiment showed that these ions were also adsorbed simultaneously on RF in the column (Fig. S4). The C/Co values were lower for Sr compared to other metals at all bed volumes indicating that the ratio of metal adsorbed to metal concentration in solution was highest for Sr as found in the batch selectivity experiment (section 3.2.6). However, the amount of Sr adsorbed on RF calculated from the breakthrough curve (0.14 meq/g) was lower than that of the co-ions (Mg 30 meq/g and Ca 5.4 meq/g) because of the much higher concentrations of these co-ions than Sr in the synthetic seawater. Despite K had much higher concentration than Sr in synthetic seawater medium, amount of K adsorbed (0.13 meq/g) was lower than Sr. This indicates that Sr has higher selectivity for adsorption than K as found in the batch selectivity experiment (section 3.2.6).

Table 2.

The values for Thomas model parameters and error analysis of the model's fit to the experimental data.

Influent metals and concentrations	Model parameters		Error analysis		
	q_0 (meq/g)	K_{Th} (mL/min. meq)	SSE	RMSE	Coefficient of determination between model values and experimental values (R^2)
(a) Sr = 10 mg/L	0.46	0.009	0.13	0.09	0.93
(b) Sr =10 mg/L, Na=20 g/L, Ca=1 g/L, Mg=2 g/L, K= 0.85 g/L	0.17	0.008	0.98	0.25	0.64
(c) Sr=10 mg/L, Na=20 g/L, K= 0.85 g/L	0.20	0.003	0.34	0.15	0.76

4. Conclusions

An RF resin synthesised by poly-condensation of formaldehyde and resorcinol followed by conditioning it with high concentration of NaOH had higher Sr adsorption capacity than RF resins conditioned with KOH and Ca(OH)$_2$. Sr adsorption on the NaOH conditioned RF increased with pH reaching a maximum value at pH 7.5-8.5. The Langmuir Sr adsorption capacity for this resin at pH 7.5-8.5 was 2.28 meq/g which is among the highest values reported in the literature for other adsorbents. The adsorption capacity for the different metals followed the order, Sr > Ca > Mg > K. The negative zeta potential of RF in the presence of Na markedly

increased with pH but the rate of increase was much lower in the presence of Sr. Sr was adsorbed by both the outer-sphere complexation and inner-sphere complexation whereas Na and K adsorption was mainly by outer-sphere complexation. Sr adsorption capacity was reduced in synthetic seawater containing high concentrations of Na, K, Ca, and Mg in both batch and column experiments. The reduction was mainly due to Ca and Mg. However, the selectivity coefficient of Sr in the presence of K, Ca, and Mg when all metals were present together, each at the same concentration, was greater than one (1.13, 1.46, and 79 with respect to Ca, Mg, and K, respectively) suggesting that Sr was selectively adsorbed on RF. 1 M NaCl was found to be an efficient reagent for the recovery of Sr adsorbed on RF and regeneration of the used RF for reuse. The study indicated that RF conditioned with NaOH is an attractive adsorbent for removing Sr from seawater, provided Ca and Mg are removed prior to the adsorption process probably by precipitating them as carbonate and hydroxide, respectively.

References

[1] P. Loganathan, G. Naidu, S. Vigneswaran, Mining valuable minerals from seawater: a critical review, Environ. Sci.: Water Res. Technol. 3 (2017) 37–53.

[2] E.E. Angino, G.K. Billings, N. Andersen, Observed variations in the strontium concentration of sea water, Chem. Geol. 1 (1966) 145–153.

[3] J.A. Ober, Strontium, US Geological Survey Mineral Commodity Summaries, US Geological Survey, 2013, pp. 156–157.

[4] B. Ma, S. Oh, W.S. Shin, S.J. Choi, Removal of Co^{2+}, Sr^{2+} and Cs^+ from aqueous solution by phosphate-modified montmorillonite (PMM), Desalination 276 (2011) 336–346.

[5] S. Singh, S. Eapen, V. Thorat, C.P. Kaushik, K. Raj, S.F. D'souza, Phytoremediation of [137]cesium and [90]strontium from solutions and low-level nuclear waste by Vetiveria zizanoides, Ecotoxicol. Environ. Safe. 69 (2008) 306–311.

[6] A. Sachse, A. Merceille, Y. Barré, A. Grandjean, F. Fajula, A. Galarneau, Macroporous LTA-monoliths for in-flow removal of radioactive strontium from aqueous effluents: application to the case of Fukushima, Microporous Mesoporous Mater. 164 (2012) 251–258.

[7] K. Shozugawa, B. Riebe, C. Walther, A. Brandl, G. Steinhauser, Fukushima-derived radionuclides in sediments of the Japanese pacific-ocean coast and various Japanese water samples (seawater, tap water, and coolant water of Fukushima Daiichi reactor unit 5), J. Radioanal. Nucl. Chem. 307 (2016) 1787–1793.

[8] M. Nagaoka, H. Yokoyama, H. Fujita, M. Nakano, H. Watanabe, S. Sumiya, Spatial distribution of radionuclides in seabed sediments off Ibaraki coast after the Fukushima Daiichi nuclear power plant accident, J. Radioanal. Nucl. Chem 303 (2015) 1305–1308.

[9] U.S. Department of Health and Human Services, Toxicological profile for strontium, Public Health Service, Agency for toxic substances and disease registry, Washington, DC, USA, 2004.

[10] V. Höllriegl, H.Z. München, Strontium in the environment and possible human health effects, in: J.O. Nriagu (Eds.), Encyclopedia of Environmental Health, Elsevier, Burlington, 2011, pp. 268–275

[11] C. Xu, J. Wang, J. Chen Solvent extraction of strontium and cesium: a review of recent progress, Solvent Extr. Ion Exc. 30 (2012) 623–650.

[12] A.D. Ebner, J.A. Ritter, J.D. Navratil, Adsorption of cesium, strontium, and cobalt ions on magnetite and a magnetite-silica composite, Ind. Eng. Chem. Res. 40 (2001) 1615–1623.

[13] S. Chegrouche, A. Mellah, M. Barkat, Removal of strontium from aqueous solutions by adsorption onto activated carbon: kinetic and thermodynamic studies, Desalination 235 (2009) 306–318.

[14] D.V. Marinin, G.N. Brown, Studies of sorbent/ion-exchange materials for the removal of radioactive strontium from liquid radioactive waste and high hardness groundwaters, Waste Manage. 20 (2000) 545–553.

[15] Z.V.P. Murthy, S. Parmar, Removal of strontium by electrocoagulation using stainless steel and aluminium electrodes, Desalination 282 (2011) 63–67.

[16] D.R. Raut, P.K. Mohapatra, V.K. Manchanda, A highly efficient supported liquid membrane system for selective strontium separation leading to radioactive waste remediation, J. Membr. Sci. 390 (2012) 76–83.

[17] P. Loganathan, S. Vigneswaran, J. Kandasamy, N.S. Bolan, Removal and recovery of phosphate from water using sorption, Crit. Rev. Environ. Sci. Tech. 44 (2014) 847–907.

[18] T.D. Small, L.A. Warren, F.G. Ferris, Influence of ionic strength on strontium sorption to bacteria, Fe (III) oxide, and composite bacteria Fe (III) oxide surfaces, Appl. Geochem. 16 (2001) 939–946.

[19] A. Ghaemi, M. Torab-Mostaedi, M. Ghannadi-Maragheh, Characterizations of strontium (II) and barium (II) adsorption from aqueous solutions using dolomite powder, J. Hazard. Mater. 190 (2011) 916–921.

[20] Q. Li, H. Liu, T. Liu, M. Guo, B. Qing, X. Ye, Z. Wu, Strontium and calcium ion adsorption by molecularly imprinted hybrid gel, Chem. Eng. J. 157 (2010) 401–407.

[21] H.J. Hong, J. Ryu, I.S. Park, T. Ryu, K.S. Chung, B.G. Kim, Investigation of the strontium (Sr (II)) adsorption of an alginate microsphere as a low-cost adsorbent for removal and recovery from seawater, J. Environ. Manage. 165 (2016) 263–270.

[22] O. Oleksiienko, I. Levchuk, M. Sitarz, S. Meleshevych, V. Strelko, M. Sillanpää, Removal of strontium (Sr^{2+}) from aqueous solutions with titanosilicates obtained by the sol–gel method, J. Colloid Interface Sci. 438 (2015) 159–168.

[23] S. Samanta, M. Ramaswamy, B. Misra, Studies on cesium uptake by phenolic resins, Sep. Sci. Technol. 27 (1992) 255–267.

[24] C. Dwivedi, A. Kumar, J.K. Ajish, K.K. Singh, M. Kumar, P.K. Wattal, P.N. Bajaj, Resorcinol-formaldehyde coated XAD resin beads for removal of cesium ions from radioactive waste: synthesis, sorption and kinetic studies, RSC Adv. 2 (2012) 5557–5564.

[25] J. Kaczvinsky, J. Fritz, D. Walker, M. Ebra, Synthesis and development of porous chelating polymers for the decontamination of nuclear waste, J. Radioanal. Nucl. Chem 91(1985) 349–360.

[26] D. Banerjee, R.A. Rao, P.K. Wattal, Separation and recovery of Cs from high activity waste simulant using resorcinol formaldehyde polycondensate resin: batch and column studies, Sep. Sci. Technol. 48 (2013) 133–139.

[27] E.A. Behrens, P. Sylvester, A. Clearfield, Assessment of a sodium nonatitanate and pharmacosiderite-type ion exchangers for strontium and cesium removal from DOE waste simulants, Environ. Sci. Technol. 32(1998) 101–107.

[28] D. Banerjee, M.A. Rao, S.K. Samanta, Evaluation of Amberlite IRC-718 chelating ion exchange resin in loading-elutionregeneration cycles for separation and recovery of strontium from alkaline radioactive waste, Solvent Extr. Ion Exch. 26 (2008) 687–698.

[29] Y. Park, Y. Lee, W.S. Shin, S. Choi, Removal of cobalt, strontium and cesium from radioactive laundry wastewater by ammonium molybdophosphate–polyacrylonitrile (AMP–PAN), Chem. Eng. J. 162 (2010) 685–695.

[30] S.K. Samanta, B.M. Misra, Ion exchange selectivity of a resorcinol-formaldehyde polycondensate resin for cesium in relation to other alkali metal ions, Solvent Extr. Ion Exch. 13 (1995) 575–589.

[31] J. Pan, X. Zou, Y. Yan, X. Wang, W. Guan, J. Han, X. Wu, An ion-imprinted polymer based on palygorskite as a sacrificial support for selective removal of strontium (II), Appl. Clay Sci. 50 (2010) 260–265.

[32] T. Nur, W.G. Shim, P. Loganathan, S. Vigneswaran, J. Kandasamy, Nitrate removal using Purolite A520E ion exchange resin: batch and fixed-bed column adsorption modelling, Int. J. Environ. Sci. Technol. 12 (2015) 1311–1320.

[33] J.J. García-Sánchez, M. Solache-Ríos, V. Martínez-Miranda, R. Enciso-Perez, N.V. Arteaga-Larios, M.C. Ojeda-Escamilla, I. Rodríguez-Torres, Experimental study of the adsorption of

fluoride by modified magnetite using a continuous flow system and numerical simulation, Process Saf. Environ. Prot. 109 (2017) 130–139.

[34] S.A. Shady, Selectivity of cesium from fission radionuclides using resorcinol–formaldehyde and zirconyl-molybdopyrophosphate as ion-exchangers, J. Hazard. Mater. 167 (2009) 947–952.

[35] C.H. Liu, Y.J. Shih, Huang, Y.H., Huang, C.P. Kinetic and thermodynamic studies for adsorptive removal of Sr^{2+} using waste iron oxide, J. Taiwan Inst. Chem. Eng. 45 (2014) 914-920.

[36] Y.J. Tu, C.F. You, Y.R. Chen, C.P. Huang, Y.H. Huang, Application of recycled iron oxide for adsorptive removal of strontium, J. Taiwan Inst. Chem. Eng. 53 (2015) 92–97.

[37] L. Sun, M. Li, M. Lin, B. Peng, J. Guo, Dispersion properties of a water-soluble phenol-formaldehyde resin, J. Disper. Sci. Technol. 30 (2009) 605–608.

[38] K.G. Varshney, V. Jain, N. Tayal, Ion Exchange kinetics of alkaline earth metals on acrylamide zirconium (IV) phosphate cation exchanger, Indian J. Chem. 41A (2002) 2318–2320

[39] P.W. Atkins, J.A. Beran, General Chemistry, 2nd ed., Scientific American Books, New York, 1992.

[40] S. Langley, A.G. Gault, A. Ibrahim, Y. Takahashi, R. Renaud, D. Fortin, I.D. Clark, F.G. Ferris, Sorption of strontium onto bacteriogenic iron oxides, Environ. Sci. Technol. 43 (2009) 1008–1014.

[41] Z. Cheng, Z. Gao, W. Ma, Q. Sun, B. Wang, X. Wang, Preparation of magnetic Fe_3O_4 particles modified sawdust as the adsorbent to remove strontium ions, Chem. Eng. J. 209 (2012) 451–457

[42] J. Marešová, M. Pipíška, M. Rozložník, M. Horník, L. Remenárová, J. Augustín, Cobalt and strontium sorption by moss biosorbent: modeling of single and binary metal systems, Desalination 266 (2011) 134–141.

[43] Y.J. Tu, C.F. You, Z. Zhang, Y. Duan, J. Fu, D. Xu, Strontium removal in seawater by means of composite magnetic nanoparticles derived from industrial sludge, Water 8 (2016) 357.

[44] J. Ryu, S. Kim, H.J. Hong, J. Hong, M. Kim, T. Ryu, I.S. Park, K.S. Chung, J.S. Jang, B.G. Kim, Strontium ion (Sr^{2+}) separation from seawater by hydrothermally structured titanate nanotubes: removal vs. recovery, Chem. Eng. J. 304 (2016) 503–510.

Supplementary data

Removal of strontium from aqueous solutions and synthetic seawater using resorcinol formaldehyde polycondensate resin

T. Nur, P. Loganathan, J. Kandasamy, S. Vigneswaran

Faculty of Engineering, University of Technology Sydney (UTS), P.O. Box 123, Broadway, NSW

2007, Australia

*Corresponding author. Tel.:+61 2 95142641, fax: +61 2 95142633.

Email: s.vigneswaran@uts.edu.au

Table S1.

Different metals adsorption by RF resin with the dose of 1g/L at different initial metals concentrations.

Metal concentration (mg/L)	Adsorption capacity (meq/g)			
	Sr	Ca	Mg	K
Sr 10	0.27			
Sr 10 + K 10	0.27			0.09
Sr 10 + K 20	0.27			0.13
Sr 10 + K 40	0.27			0.22
Sr 10 + Mg 10	0.26		0.90	
Sr 10 + Mg 20	0.25		0.93	
Sr 10 + Mg 40	0.24		1.04	
Sr 10 + Ca 10	0.25	0.37		
Sr 10 + Ca 20	0.24	0.46		
Sr 10 + Ca 40	0.23	0.52		

Table S2.

Distribution coefficients (K_d) of the metals and the selectivity coefficient (K_s) of Sr with respect to other metals

Metal ions	The distribution coefficient, K_d (L/g)	The selectivity coefficient of Sr, K_s
Sr	0.079	
Ca	0.070	1.13
Mg	0.054	1.46
K	0.001	79.0
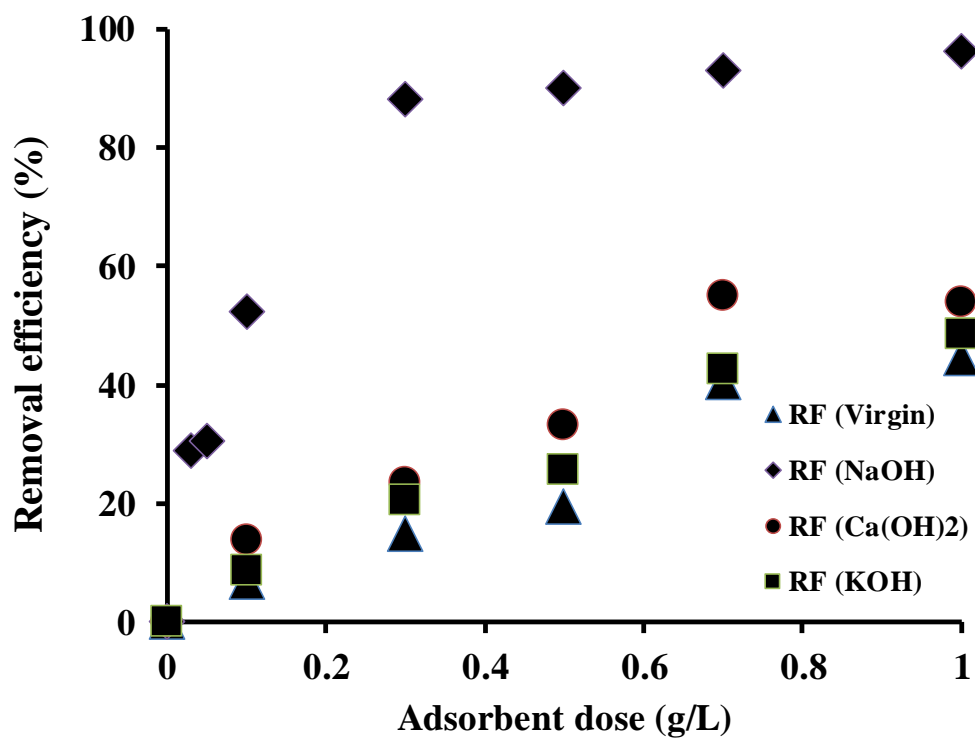
Fig. S1. Sr adsorption isotherm of RF resin conditioned with different metal hydroxides (initial

Sr concentration 10 mg/L, adsorbents doses of 0.1 – 1.0 g/L, pH =7.5 - 8.5).
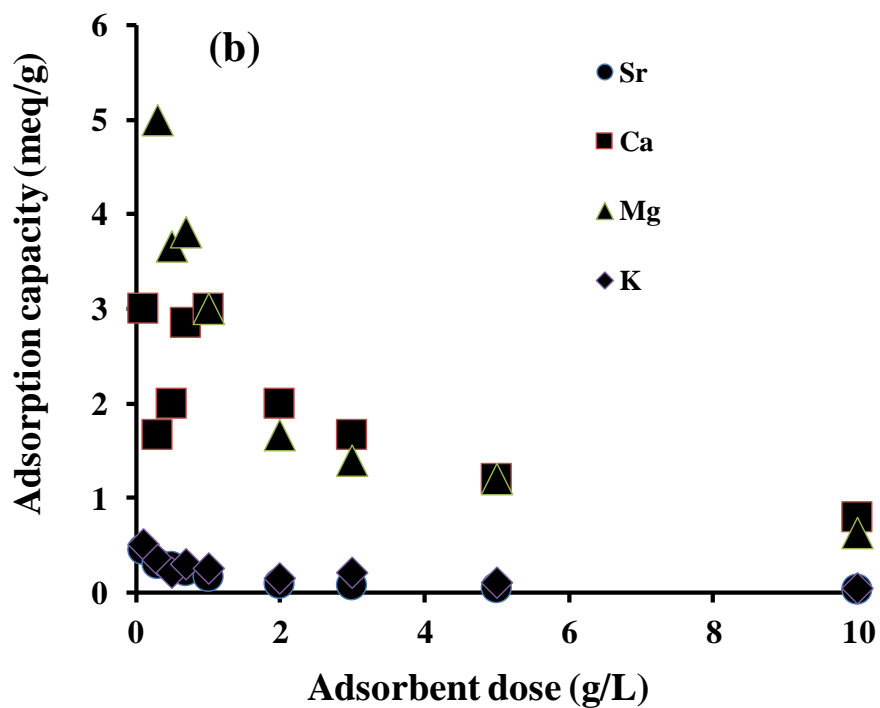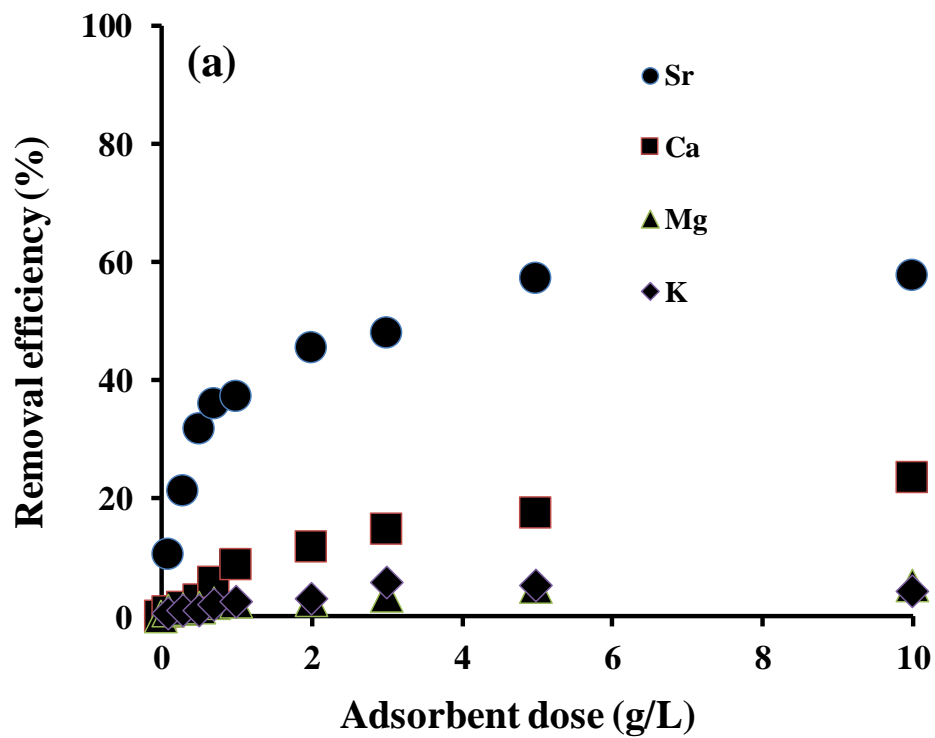
Fig. S2. (a) Removal efficiency and (b) adsorption capacity of Sr, Ca, Mg and K by RF resin

in synthetic seawater medium with different doses of adsorbent (Seawater concentration, Na =

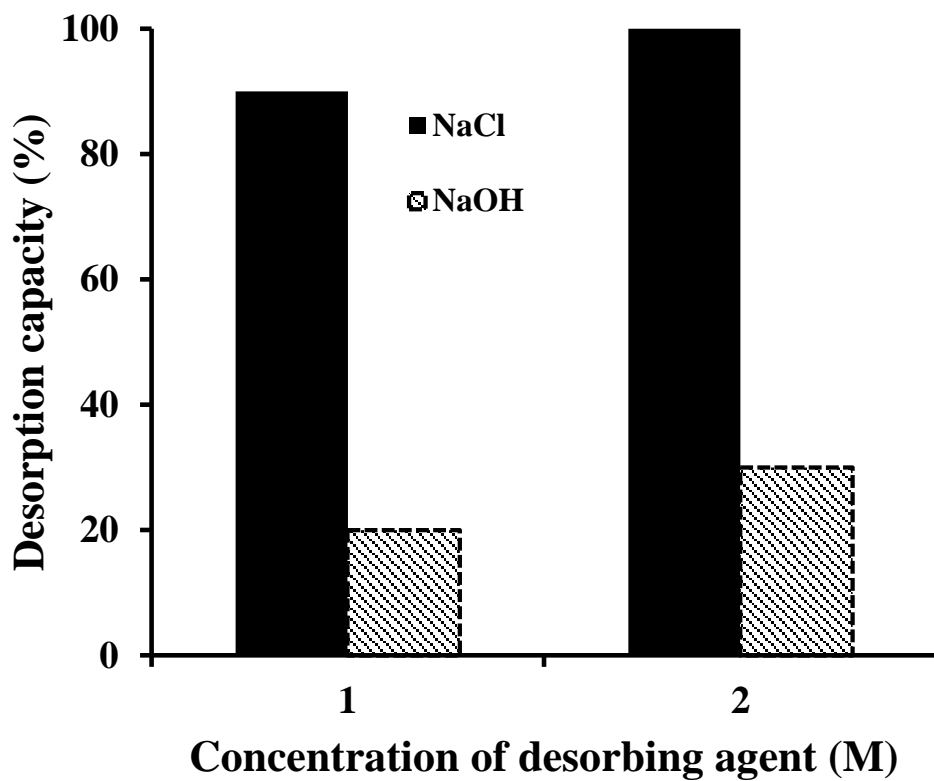20 g/L, Ca = 1 g/L, Mg = 2 g/L, K = 0.85 g/L, Sr = 0.01 g/L).

Fig. S3. Effect of different desorbing agents on Sr desorption from RF resin containing adsorbed Sr.
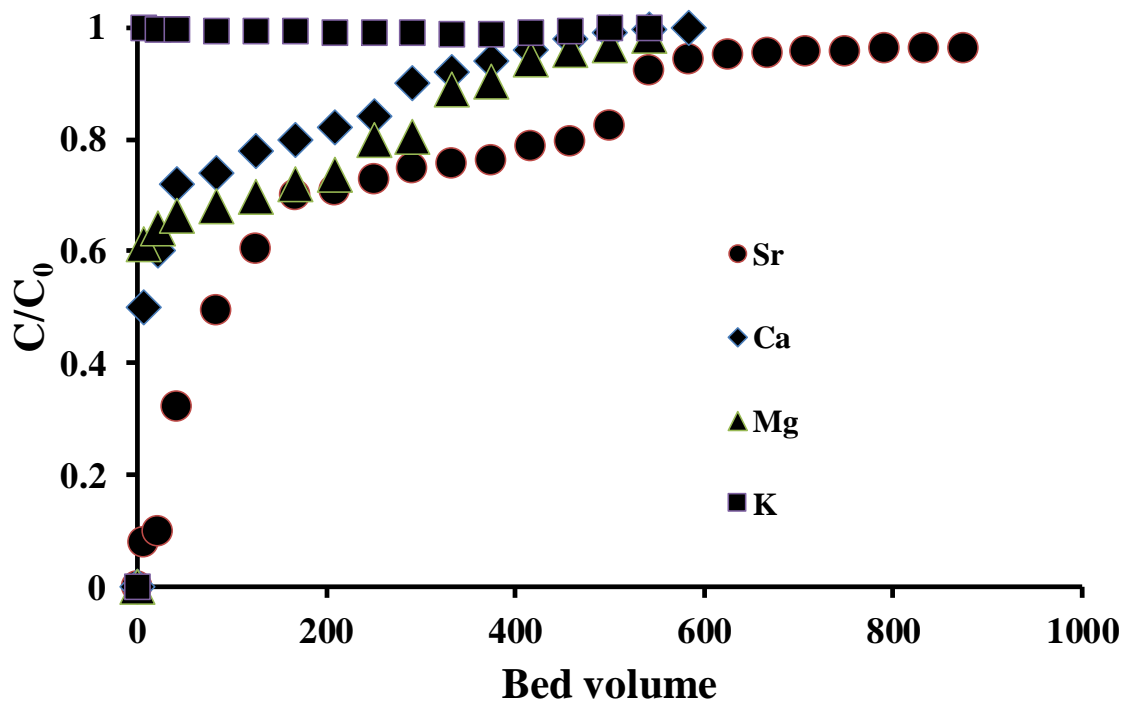
Fig. S4. Breakthrough curves for all metals adsorption using RF resin for synthetic seawater (filtration velocity 2.5 m/h, bed height 6 cm) (Seawater concentration, Na = 20 g/L, Ca = 1 g/L, Mg = 2 g/L, K = 0.85 g/L, Sr = 0.01 g/L).
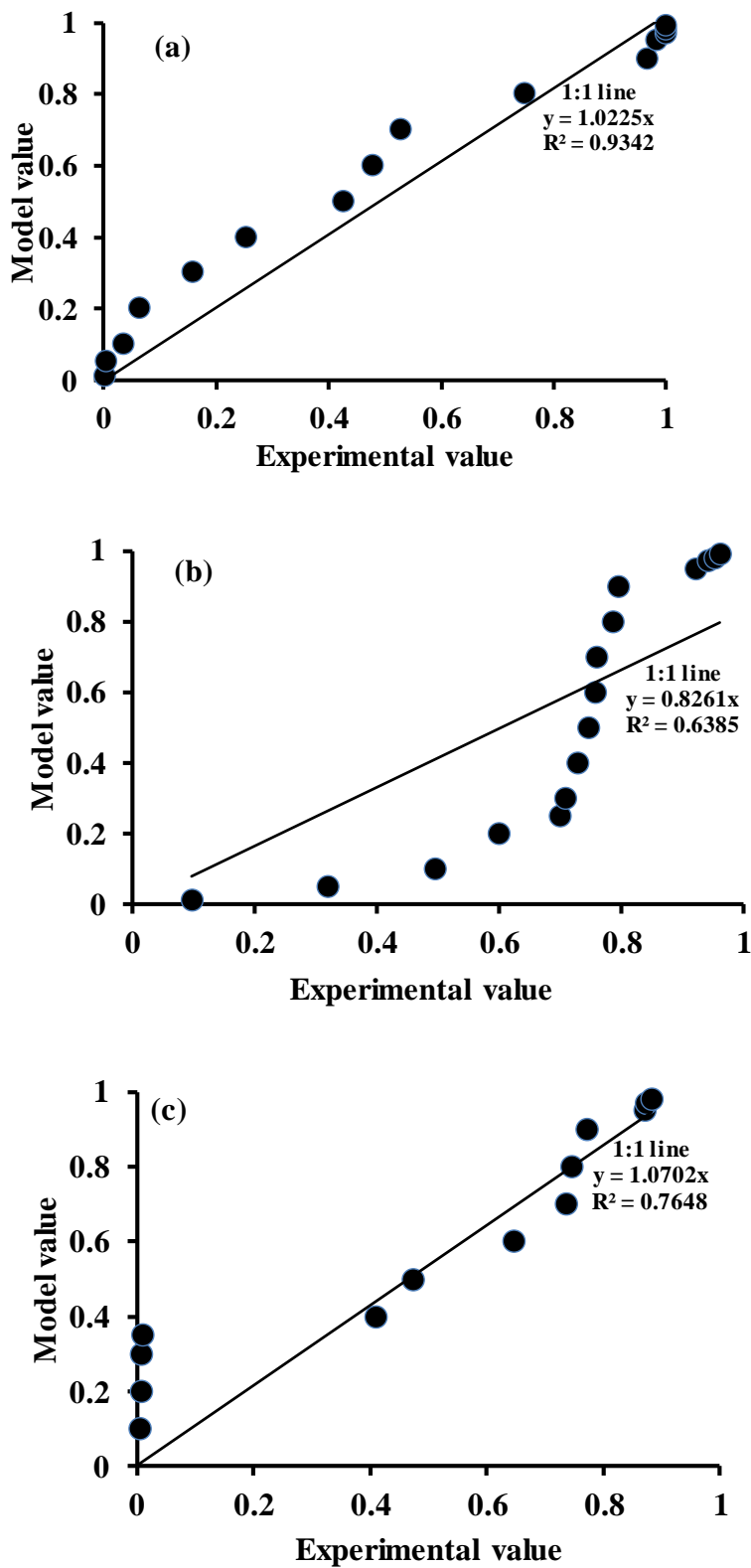
Fig. S5. Relationship between experimental and model predicted C/C_0 values. Data fitted to the regression equation, $y = mx$.